Scientific Research Publishing

Structural, Spectral (IR and UV/Visible) and Thermodynamic Properties of Some 3d Transition Metal(II) Chloride Complexes of Glyoxime and Its Derivatives: A DFT and TD-DFT Study

Ludovid Ngouo Nogheu[1], Julius Numbonui Ghogomu[1*], Desire Bikele Mama[2], Nyiang Kennet Nkungli[1], Elie Younang[3], Shridhar Ramachandra Gadre[4]

[1]Department of Chemistry, Faculty of Science, University of Dschang, Dschang, Cameroon
[2]Department of Chemistry, Faculty of Science, University of Douala, Douala, Cameroon
[3]Department of Inorganic Chemistry, Faculty of Science, University of Yaounde I, Yaounde, Cameroon
[4]Department of Chemistry, Indian Institute of Technology Kanpur, Kanpur, India
Email: *ghogsjuju@hotmail.com

Abstract

Metal complexes bearing vic-dioxime ligands have been extensively used as analytical and biochemical reagents, and are well-known antimicrobial agents. Herein is reported a DFT study on the molecular structures, thermodynamic properties, chemical reactivity and spectral properties of some 3d metal(II) chloride complexes of glyoxime. The functionals B3LYP and CAM-B3LYP have each been used in conjunction with LANL2DZ for the metal(II) ions (Fe^{2+}, Co^{2+}, Ni^{2+} and Cu^{2+}) and the Pople-style basis set 6-31G+(d,p) for the rest of the elements, to perform theoretical calculations. The metal complexation abilities of the glyoxime ligands studied in this work have been evaluated on the basis of metal-ligand binding energies. These ligands were found to have high affinities towards Ni(II) and Fe(II) ions, and all complexation reactions were found to be thermodynamically feasible. Ligand-to-metal electron donations in the complexes studied have been revealed by natural population analysis. The fully optimized geometries of the complexes have adopted square planar structures around the central metal ions. On the basis of orbital composition analysis, the UV-Vis electronic absorption bands of these molecules have been attributed mainly to MLCT, LMCT and d-d electronic transitions involving metal-based orbitals.

Keywords

Glyoxime Complexes, DFT, Binding Energy, Electronic Absorption

1. Introduction

The interaction of a central metal with surrounding ligands (atoms, ions or molecules) has been of significant interest in coordination chemistry. In the past decades, the coordination chemistry of transition metal complexes bearing oxime ligands has been a subject of intense studies owing to their applications in many scientific domains like biomedical and electrochemistry. Synthesis of Co(III), Ni(II) and Cu(II) complexes based on two glyoxime derivatives namely: dianiline glyoxime and disulfanilamide glyoxime were envisaged and were found to be effective as stimulators in biosynthetic processes of enzymes in some fungi strains [1]. In one review, the synthesis of phenolic oximes and their complexes were reported to be more effective in commercial metal recovery processes based on solvent extraction as a result of their remarkable stability [2]. These studies have been motivated by the fact that oximes are important analytical, biochemical, and antimicrobial agents. They have equally attracted much attention due to their structural features and their uses as liquid crystals and dyes [3]-[6].

Vicinal dioxime derivatives act as amphoteric ligands due to the presence of weak acidic -OH groups and basic -C = N groups. As such, they are capable of forming highly stable complexes with most transition metals in the periodic table. The exceptional stability and electronic properties displayed by these complexes are attributable to their hydrogen bond-stabilized planar structures [7]-[9]. These complexes have been extensively used for various purposes owing to their high stability, suitability as model compounds for vitamin B12 and as chelators in trace metal analysis [10] [11]. These compounds also play a significant role in domains such as stereochemistry, structure isomerism, spectroscopy, model systems of biochemical interest, cation exchange and ligand exchange chromatography, analytical chemistry, catalysis, stabilizers, polymers, photography, technological improvement, pigments, and dyes [12]-[16]. Furthermore, they have been identified as compounds capable of columnar stacking, which may enhance semiconducting properties [17]. It is well established that different ligand types can affect the stabilities and properties of complexes in various ways. As such, the substitution of some dioxime groups or fragments can significantly modify the structures and stability of its complexes. The stability resulting from metal ion chelation by glyoxime ligands in the complexes currently studied is also dependent on the type of central metal ion present. This research is geared toward facilitating the construction of new vicinal glyoxime derivatives capable of forming very stable 3d metal(II) complexes, and which can be used in trace metal analysis.

After a detailed literature survey, we have found to the best of our knowledge that very little theoretical studies have been carried out on glyoxime complexes till date [18] [19]. Moreover, spectroscopic and X-ray crystallographic studies on these molecules have not been performed. In the present paper, density functional theory (DFT) studies have been undertaken on some 3d metal(II) chloride glyoxime complexes. Specifically, the structural, thermodynamic and spectral properties as well as the chemical reactivity of these compounds have been studied. Quantum chemical computations have been used in this research endeavor because they have become an established method for the

prediction of novel structures and properties in the last decades. Interestingly, they constitute a powerful tool for analyzing the properties of coordination compounds, and are widely used nowadays to complement experimental works.

2. Computational Procedure

All theoretical calculations were performed using the Gaussian 09 program package [20]. Molecular geometries were optimized in vacuum using the B3LYP exchange-correlation hybrid functional in conjunction with the LANL2DZ basis set for the central metal ions and the Pople-style basis set 6-31+G(d,p) for the elements: C, H, O, Cl and N. All optimized geometries were characterized by vibrational frequency calculations at the same level of theory as that used for geometry optimization, and only real frequencies were found confirming the optimized geometries as minima on their potential energy surfaces. For all theoretical calculations, we adopted the restricted closed-shell model for the closed-shell Ni^{2+} and Fe^{2+} complexes and the unrestricted model for the open-shell Co^{2+} and Cu^{2+} complexes. All complexes were treated as low spin species. Natural population analysis (NPA) calculations were performed using the NBO 3.1 program as implemented in the Gaussian 09 package [20] at the same theoretical level as that used for geometry optimization calculations. TD-DFT calculations were performed on the optimized ground state geometries of the molecules under investigation, in order to simulate their absorption spectra [21] [22]. In these calculations, excitations to the first 20 singlet excited states were considered, and the CAM-B3LYP functional was used together with the same basis set as that used for geometry optimization.

3. Results and Discussion

3.1. Molecular Geometry

The square planar schematic structures of the investigated 3d metal glyoxime complexes, showing atomic numbering are presented in **Figure 1**. The different structures have been obtained by changing the central metal (M = Fe^{2+}, Co^{2+}, Ni^{2+} and Cu^{2+}) and the alkyl radical (R = H, $-CH_3$ and $-C_6H_5$). The geometric parameters (bond lengths, bond
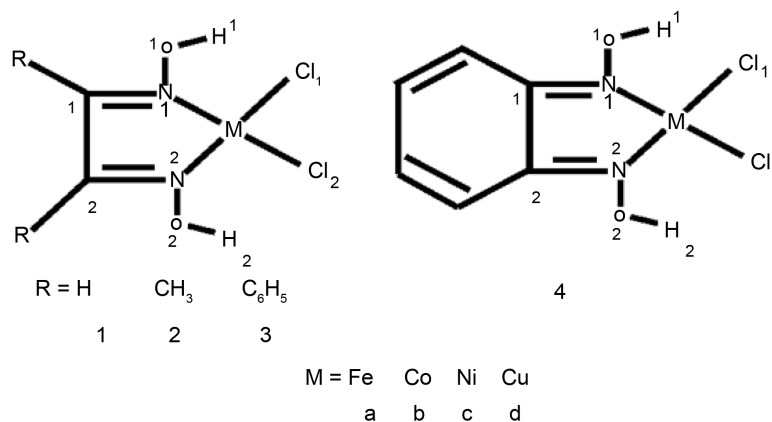
Figure 1. Schematic structures of investigated complexes.

angles, and dihedral angles) of the ground state geometries of the molecule studied optimized at the DFT/6-31+G(p,d)/(LANL2DZ for metal ions) level, are listed in Table 1.

Table 1. Main optimized bond lengths (Å), bond angles (°) and dihedral angles (°) of metal 3d glyoxime complexes at B3LYP/ 6-31+G(d,p) with LANL2DZ for metal(II).

Molecules	$d(C_1-N_1)$	$d(C_2-N_2)$	$d(C_1-C_2)$	$d(M-N_2)$	$d(M-N_1)$	$d(N_1-O_1)$	$d(N_2-O_2)$	$d(M-Cl_1)$	$d(M-Cl_2)$	$d(O_1-H_1)$	$d(O_2-H_2)$
1a	1.317	1.317	1.418	1.892	1.892	1.359	1.359	2.209	2.209	0.991	0.991
1b	1.299	1.299	1.443	1.930	1.930	1.352	1.352	2.209	2.209	0.995	0.995
1c	1.292	1.292	1.456	1.929	1.929	1.346	1.346	2.198	2.198	0.999	0.999
1d	1.286	1.286	1.468	2.092	2.092	1.346	1.346	2.263	2.263	0.997	0.997
2a	1.324	1.324	1.441	1.877	1.877	1.366	1.366	2.220	2.220	0.992	0.992
2b	1.303	1.302	1.469	1.915	1.924	1.360	1.360	2.217	2.217	0.996	0.996
2c	1.302	1.302	1.480	1.922	1.922	1.355	1.355	2.204	2.204	0.998	0.998
2d	1.291	1.290	1.494	2.063	2.075	1.356	1.356	2.266	2.270	0.996	0.996
3a	1.328	1.328	1.450	1.876	1.770	1.365	1.365	2.221	2.221	0.993	0.993
3b	1.308	1.308	1.479	1.916	1.916	1.359	1.359	2.218	2.218	0.996	0.996
3c	1.302	1.302	1.492	1.915	1.915	1.354	1.354	2.205	2.205	0.999	0.999
3d	1.296	1.296	1.504	2.045	2.045	1.362	1.362	2.298	2.298	0.987	0.987
4a	1.366	1.366	1.426	1.810	1.810	1.357	1.357	2.228	2.228	0.994	0.994
4b	1.319	1.319	1.461	1.901	1.901	1.357	1.357	2.213	2.213	0.994	0.994
4c	1.308	1.308	1.473	1.916	1.916	1.351	1.351	2.201	2.201	0.998	0.998
4d	1.301	1.301	1.488	2.072	2.072	1.350	1.350	2.268	2.268	0.997	0.997

	$d(H_1-Cl_1)$	$d(H_2-Cl_2)$	$\varangle(Cl_1-M-Cl_2)$	$\varangle(N_1-M-N_2)$	$\varangle(O_1-H-Cl_1)$	$\varangle(O_2-H_2-Cl_2)$	$\varangle(Cl_1-M-N_2)$	$\Phi(Cl_1-M-N_1-C_1)$	$\Phi(M-N_1-C_1-C_2)$
1a	2.170	2.170	97.537	81.403	138.997	138.997	171.93	−179.998	0.0026
1b	2.143	2.143	98.004	80.785	141.100	141.100	171.390	−179.994	0.0008
1c	2.112	2.112	97.271	80.943	142.176	142.176	171.836	−179.999	0.000
1d	2.174	2.174	105.963	75.999	144.786	144.786	165.018	−179.996	−0.001
2a	2.139	2.139	97.189	80.763	140.723	140.723	171.787	180.000	0.000
2b	2.108	2.122	97.582	80.189	143.262	142.306	171.411	−179.987	−0.001
2c	2.085	2.098	96.768	80.334	144.045	143.099	171.895	−179.983	−0.034
2d	2.143	2.153	104.809	75.584	146.729	145.838	165.500	−179.980	−0.006
3a	2.109	2.109	96.254	81.053	142.191	142.190	172.398	−179.046	−1.980
3b	2.090	2.090	96.717	80.282	144.037	144.036	171.774	−179.057	−3.410
3c	2.063	2.063	95.941	80.411	144.867	144.867	172.230	−178.649	−4.120
3d	2.209	2.209	100.022	76.836	145.735	145.735	168.406	−175.926	−9.933
4a	2.110	2.110	95.050	84.033	139.431	139.436	174.494	−179.994	0.001
4b	2.130	2.130	96.668	81.852	141.140	141.159	172.588	−179.985	0.002
4c	2.101	2.102	96.654	81.487	142.431	142.431	172.411	−179.992	0.006
4d	2.152	2.151	105.004	76.575	145.558	145.580	165.777	−179.993	0.011

These values ought to be compared with those obtained experimentally, but X-ray crystallographic data is not available in the literature for these complexes. It is clear from the values in Table 1 that all complexes studied are nearly symmetric, and possess two intra-molecular hydrogen bonds (O-H … Cl) each, between the hydrogens of the oxime group and the chloride ligands. These hydrogen bonds contribute in stabilizing the complexes and in maintaining a square planar geometry around their central metal ions.

It is evident from Table 1 that the M-Cl and M-N bond lengths in Fe(II) and Ni(II) complexes are shorter than corresponding bond lengths in Cu(II) and Co(II) complexes the greatest discrepancies being 0.093 Å for M-Cl between 3d and 3c, and 0.2 Å for M-N between 1d and 1a. This indicates that the ligands (glyoxime and chloride ions) interact more strongly with Fe(II) and Ni(II) ions than with Cu(II) and Co(II) ions. In almost all complexes studied, the greatest metal-ligands bond lengths are present in the Cu(II) complexes. It can be seen that the azomethine (C = N) bond lengths decrease with an increase in atomic number of the central metal ions within the 3d period, with calculated differences of about: 0.031 Å for 1a and 1d, 0.033 Å for 2a and 2d, 0.032 Å for 3a and 3d and 0.065 Å for 4a and 4d. The values of the bond angle Cl-M-Cl range from 95.05° to 105.963° in all complexes studied, and the largest values: 105.963°, 104.809°, 100.022° and 105.004° for 1d, 2d, 3d and 4d respectively, correspond to copper complexes while the smallest values: 97.271°, 96.768°, 95.941° and 96.654° for 1c, 2c, 3c and 4c respectively correspond to nickel complexes. Values of the dihedral angle Cl_1-M-N_1-C_1 are around −180° for all the complexes, except 3d for which the value is −175.927°. This shows that the optimized geometries of all complexes investigated in this research endeavor are nearly square planar around their respective central metal ions.

3.2. Thermodynamic Properties

In order to investigate thermodynamic properties of complexation reactions, statistical thermodynamic calculations were carried out at 1 atm and 298.15 K. To investigate the stability of the complexes studied, the thermodynamic parameters: binding energy (ΔE_{int}), Gibbs free energy ($\Delta G°$) and enthalpy ($\Delta H°$) of formation were calculated.

3.2.1. Complexation Energy

The complexation ability of the ligands with different metal cations is characterized by their binding energy as defined in Equation (1).

$$\Delta E = E_{complex} - \left(E_{ligand} + E_{metal} + 2E_{Cl} \right) \tag{1}$$

where $E_{Complex}$, E_{Ligand}, $E_{Metal(II)}$ and E_{Cl} are respectively the thermal energy of complex, free glyoxime ligand, free metal ions and free chloride ligands.

A large variation in the complexation energies is clear from Table 2. The binding energies are negative in all cases, implying that the complexation reactions are highly favorable. For all the ligands studied, the most negative complexation energy values have been obtained for the formation of the Ni(II) complexes whereas least negative

Table 2. Main energetical parameters of metal 3d glyoximes complexes in Kcal/mol at B3LYP/ 6-31+G(d,p) with LANL2DZ for metal(II).

Molecules	ΔG_{298}^{0}(react)	ΔH_{298}^{0}(react)	ΔE(react)
1a	−644	−670	−669
1b	−635	−661	−660
1c	−674	−700	−698
1d	−626	−651	−649
2a	−644	−671	−669
2b	−635	−662	−660
2c	−675	−702	−700
2d	−626	−653	−651
3a	−636	−664	−662
3b	−628	−655	−654
3c	−667	−695	−693
3d	−634	−660	−658
4a	−660	−686	−684
4b	−643	−669	−668
4c	−680	−706	−705
4d	−631	−656	−654

values have been obtained for the formation of the Cu(II) complexes. Hence, the ligands exhibit their greatest affinity toward the Ni(II) ion and the least toward the Cu(II) ion. For instance, the complexation energy for the formation of 1d is higher than that of formation of 1c by 49 kcal·mol^{-1}. Generally, more negative complexation energies are more thermodynamically favored. Based on this fact, it can be concluded that the formation of the Ni(II) complexes is most favorable of all the complexes investigated. It is worthy of note that the formation processes for the complexes bearing ligand 4 are most favored.

3.2.2. Gibbs Free Energy and Enthalpy Change

Besides binding energies, the standard complexation Gibbs free energy (ΔG°) and enthalpy change (ΔH°) were also calculated using Equations (2) and (3) and the results are presented in Table 2.

$$\Delta G^{\circ} = \Delta G_{complex}^{\circ} - \left(\Delta G_{ligand}^{\circ} + \Delta G_{metal}^{\circ} + 2\Delta G_{Cl}^{\circ} \right) \tag{2}$$

$$\Delta H^{\circ} = \Delta H_{complex}^{\circ} - \left(\Delta H_{ligand}^{\circ} + \Delta H_{metal}^{\circ} + 2\Delta H_{Cl}^{\circ} \right) \tag{3}$$

It is clear from Table 2 that the complexation Gibbs free energy change for the formation of all complexes investigated is negative, showing that the process is thermodynamically feasible at ambient temperature for each complex. The formation processes for the nickel complexes (1c, 2c, 3c, 4c) have been found to be the most exergonic and,

therefore, the most favored compared to the formation of the other complexes. Similarly, the enthalpies of the complexation reactions that yield the complexes studied have been found to be negative which is a clear indication that these reactions are highly exothermic.

3.3. Electronic Properties

3.3.1. Natural Population Analysis (NPA)

The NPA charges on the metal(II) ions in the complexes investigated are listed in Table 3. The positive charge on each metal ion in the complexes is less than +2, the charge on the free state metal ion, whereas the magnitudes of the negative charges on the chloride ions in the complexes is lower than −1, the charge on the free state chloride ion. This result indicates that electron transfer from the ligands to the metal ions occurred during the formation of the coordination bonds. This charge transfer is greatest for the Fe(II), Ni(II) and Co(II) complexes and least for the Cu(II) complexes. From this observation, it can be concluded that the metal-ligand bonds in the Fe(II) Ni(II) and Co(II) complexes are stronger than those in the Cu(II) complexes. This is corroborated

Table 3. Variation of natural population atomic charges (e) at B3LYP/6-31+G(d,p) with LANL2DZ for metal(II).

Molecules	M	Cl_1	Cl_2	N_1	N_2	O_1	O_2	C_1	C_2	H_1	H_2
1	-	-	-	−0.12946	−0.05480	−0.63148	−0.56382	−0.04738	−0.11855	0.53571	0.49630
1a	0.37074	−0.34660	−0.34660	−0.09933	−0.09933	−0.53319	−0.53319	0.00033	0.00033	0.52905	0.52905
1b	0.46007	−0.39576	−0.39576	−0.10306	−0.10306	−0.53038	−0.53038	0.00753	0.00753	0.52923	0.52923
1c	0.40726	−0.38906	−0.38906	−0.08747	−0.08747	−0.52606	−0.52606	0.00923	0.00924	0.52805	0.52805
1d	0.72555	−0.48898	−0.48898	−0.14004	−0.14004	−0.53103	−0.53103	0.00954	0.00954	0.53189	0.53189
2	-	-	-	−0.13289	−0.13289	−0.61469	0.51882	0.18622	0.18622	0.51882	0.51882
2a	0.36531	−0.36627	−0.36627	−0.09941	−0.09941	−0.54727	−0.54727	0.21806	0.21806	0.52897	0.52897
2b	0.45630	−0.40887	−0.40947	−0.10859	−0.10897	−0.54964	−0.54711	0.22685	0.22685	0.52814	0.52814
2c	0.40617	−0.40062	−0.40004	−0.09617	−0.09557	−0.54387	−0.54638	0.22851	0.22804	0.52797	0.52709
2d	0.72771	−0.49620	−0.49765	−0.15248	−0.15187	−0.55224	−0.55080	0.22756	0.22794	0.53073	0.53134
3	-	-	-	−0.14296	−0.04334	−0.62093	−0.54271	0.13935	0.07813	0.53767	0.50029
3a	0.37099	−0.36471	−0.36468	−0.09323	−0.09297	−0.54174	−0.54176	0.22012	0.21845	0.52582	0.52582
3b	0.45920	−0.40725	−0.40728	−0.10386	−0.10359	−0.54208	−0.54210	0.22824	0.22662	0.52554	0.52554
3c	0.40843	−0.39868	−0.39867	−0.09091	−0.09063	−0.53927	−0.53930	0.22940	0.22780	0.52433	0.52433
3d	0.73010	−0.50412	−0.50412	−0.15355	−0.15355	−0.54451	−0.54451	0.23284	0.23284	0.53357	0.53357
4	-	-	-	−0.13592	−0.14087	−0.60406	−0.58988	0.17596	0.20040	0.52151	0.51776
4a	0.31307	−0.35301	−0.35295	−0.05147	−0.05145	−0.52723	−0.52723	0.14946	0.14946	0.52840	0.52838
4b	0.46580	−0.39199	−0.39199	−0.09457	−0.09457	−0.53871	−0.53869	0.17451	0.17452	0.52943	0.52943
4c	0.41231	−0.39118	−0.39112	−0.07825	−0.07823	−0.53415	−0.53415	0.17752	0.17753	0.52857	0.52854
4d	0.72930	−0.49416	−0.49411	−0.13332	−0.13358	−0.53847	−0.53856	0.17737	0.17723	0.53207	0.53203

by the complexation energies (Table 2) which have shown that the glyoxime and chloride ligands have a higher affinity for Fe(II) Ni(II) and Co(II) ions than the Cu(II) ion. From the foregoing results, it is clear that coordinate bonding is responsible for complex formation, and ligand to metal ion charge transfer is the underlying mechanism.

3.3.2. Reactivity Descriptors

The highest occupied molecular orbital (HOMO) and lowest unoccupied molecular orbital (LUMO) are very important parameters for quantum chemistry. The frontier orbital gap helps to characterize the chemical reactivity and kinetic stability of molecules. A molecule with a small frontier orbital gap is more polarizable and is generally associated with a high chemical reactivity, low kinetic stability and is also termed soft molecule. The eigenvalues of the HOMO and LUMO as well as their energy gap reflect the chemical reactivity of a molecule. A large HOMO-LUMO energy gap has been associated with high stability of molecules [23]. The chemical potential (μ), global hardness (η) and electrophilicity (w) are global descriptors which indicate the overall stability of a chemical system [24]-[27].

The values of some global reactivity descriptors investigated in this paper are presented in Figure 2 (Table 4). It can be seen from this table that the largest HOMO-LUMO energy gaps (ΔE_{H-L}) and chemical hardness (η) values correspond to the Cu(II) complexes (1d, 2d, 3d and 4d) and the Co(II) complexes (1b, 2b, 3b and 4b), indicating that they are kinetically more stable and less reactive than the rest of the complexes. It is also observed in Figure 3 that Fe^{2+} complexes are the most reactive complexes in each series with the lower value of chemical hardness. The other reactivity descriptors presented in this figure have shown the same reactivity trend for these complexes (Table 4).
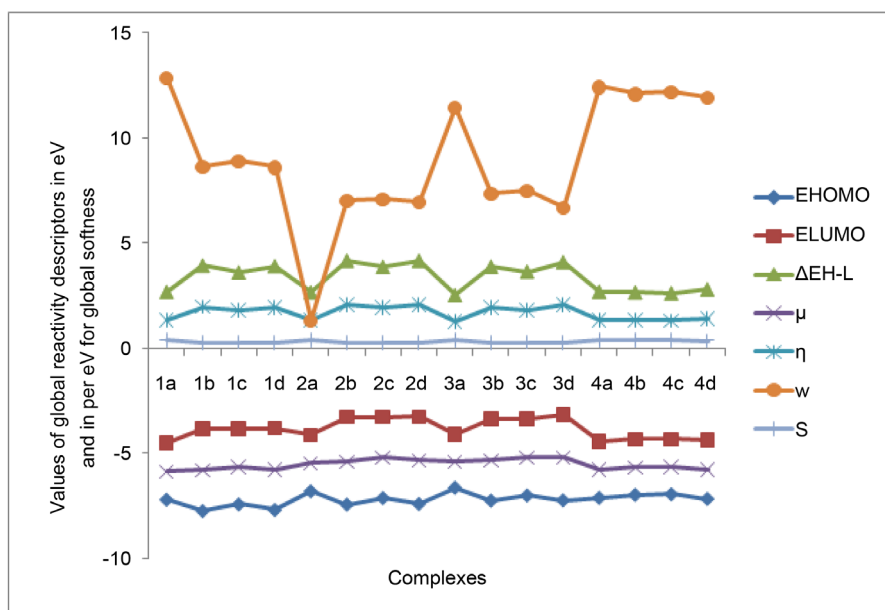
Figure 2. Superposition of the global reactivity descriptors of the systems in eV except those of global softness which are in eV^{-1}, calculated at B3LYP/6-31+G(d,p) with LANL2DZ for metal(II).

Table 4. Values of the global reactivity descriptors of the systems in eV except those of global softness which are in eV^{-1}, calculated at B3LYP/6-31+G(d,p) with LANL2DZ for metal(II).

Molecules	E_{HOMO}	E_{LUMO}	ΔE_{H-L}	μ	η	w	S
1a	−7.22	−4.53	2.68	−5.87	1.34	12.85	0.37
1b	−7.76	−3.85	3.91	−5.80	1.96	8.60	0.26
1c	−7.44	−3.85	3.59	−5.65	1.79	8.89	0.28
1d	−7.71	−3.83	3.88	−5.78	1.94	8.59	0.26
2a	−6.82	−4.15	2.66	−5.48	1.33	1.30	0.38
2b	−7.45	−3.31	4.14	−5.38	2.07	6.99	0.24
2c	−7.14	−3.30	3.85	−5.22	1.92	7.09	0.26
2d	−7.42	−3.28	4.14	−5.35	2.07	6.92	0.24
3a	−6.65	−4.12	2.53	−5.39	1.26	11.47	0.40
3b	−7.26	−3.40	3.86	−5.33	1.93	7.36	0.26
3c	−7.02	−3.40	3.63	−5.21	1.81	7.48	0.28
3d	−7.25	−3.18	4.07	−5.22	2.04	6.69	0.25
4a	−7.13	−4.44	2.69	−5.78	1.34	12.42	0.37
4b	−6.99	−4.34	2.66	−5.67	1.32	12.09	0.38
4c	−6.96	−4.34	2.62	−5.65	1.31	12.18	0.38
4d	−7.18	−4.38	2.80	−5.78	1.40	11.91	0.36
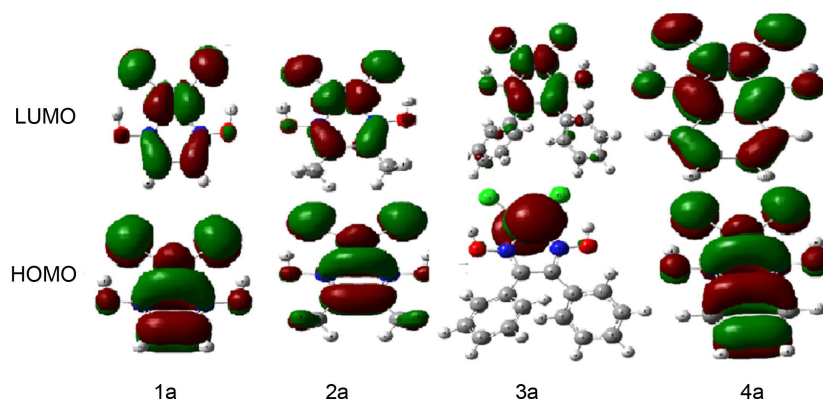
Figure 3. Picture of the HOMO-LUMO orbitals for Fe^{2+} complexes.

3.4. Infra-Red Spectroscopy

To the best of our knowledge, no IR spectral data is available in the literature for the complexes investigated in this research endeavor. The DFT/B3LYP method in conjunction with a doubly split valence basis set along with diffuse and polarization functions, 6-31+G(d,p) and LANL2DZ for the central metal(II) ions was used to calculate harmonic vibrational frequencies of the glyoximes complexes studied. IR frequencies of two complexes (1a' and 1b') were also calculated using different basis set (B3LYP/6-31+G(d,p)/SDD for metal ion) with same method in order to study the effect of basis set in

the frequency calculation. The Gauss View 5.0.8 molecular visualization program was used to perform the IR vibrational band assignments for the molecules. Although experimentally determined IR vibrational frequencies were not available for these molecules, the calculated values were still scaled down because the DFT/B3LYP method tends to overestimate normal mode frequencies due to a combination of electron correlation effects and basis set deficiencies [28]. Scaling factor for B3LYP/LANL2DZ level is 0.9978 [29]. Given the fact that this factor is very close to unity, coupled with the fact that LANL2DZ has only been used for the central metal ions, the scale factor for B3LYP/6-31+G(d,p) with numerical value 0.9614 was used for same reason [29]-[31] to scale down the computed IR frequencies. Also, it is worth noting that in a preliminary study, the IR frequencies were calculated at B3LYP/6-31+G(d,p)/(SDD for metal ions) for some of the complexes in order to compared with those calculated at B3LYP/6-31+G(d,p)/(LANL2DZ for metal ions) and very little discrepancies were observed with the calculated frequencies.

IR vibrations of the OH group are generally found to be most sensitive to the environment. As such, they show pronounced shifts in the spectra of the hydrogen-bonded species. The optimum absorption region of non-hydrogen bonded or a free hydroxyl group is 3550 - 3700 cm^{-1} [32]. In the case of their presence in a molecule, intra and intermolecular hydrogen bonding reduces the O-H stretching band to 3000 - 3550 cm^{-1} region [33]. In the complexes studied the O-H stretching band are found between 3082 - 3303 cm^{-1}, signifying that all O-H groups in the complexes studied are engaged in intramolecular hydrogen bonding with the chloride ligands. The simulated IR spectra have also shown an intense and relatively sharp band in the range 1426 - 1554 cm^{-1} assignable to the stretching C-C vibrations of glyoxime moiety of the complexes. Compared to the C-C stretching vibrations in the free glyoxime ligands (1234 - 1355 cm^{-1}), these vibrations have shifted toward regions of very large wavelengths upon complexation, showing that the electron density in C-C bond is increased by transition metal complexation by the stated ligands.

As a general observation in Table 5, significant shifts in IR vibrations occurred for the C = N bonds, implying that their vibrations are the most affected by complexation since their vibrational frequencies in the complexes significantly differ from those in the free ligands. The coordination of the vic-dioxime ligands to the metal center via the two nitrogen atoms is expected to reduce the electron density in the azomethine link and thus lowers the C = N absorption frequency. The C = N peaks of the complexes were indeed shifted to lower frequencies indicating the coordination of the azomethine nitrogen to the metal ions.

3.5. Absorption Spectra Analysis

The absorption spectral simulation of 3d metal(II) glyoximes complexes have been performed using Time-Dependent DFT calculations at the Cam-B3LYP/6-31G+(d,p)/ (LanL2DZ for metal(II) ions) levels of theory in gas phase. The calculated absorption energy, corresponding oscillator strength and orbital coefficients are summarized in

Table 5. Calculated vibrational frequencies (cm^{-1}) at B3LYP/6-31+G(d,p) with LANL2DZ for metal(II).

Molecules	$\tilde{v}$(O-H)	$\tilde{v}$(C = N)	$\tilde{v}$(N-O)	$\tilde{v}$(C-C)	$\tilde{v}$(C-H)
1	3331 - 3668	1558 - 1638	863	1307	3045 - 3055
1a	3246 - 3252	1500 - 1566	1091 - 1130	1439	3110 - 3119
1a'	3268 - 3274	1500 - 1568	1090 - 1124	1441	3108 - 3117
1b	3166 - 3179	1569	1115 - 1136	1457	3097 - 3107
1b'	3183 - 3196	1565 - 1617	1109 - 1132	1452	3097 - 3108
1c	3107 - 3126	1602 - 1640	1138 - 1148	1462	3093 - 3103
1d	3151 - 3169	1608 - 1661	1135 - 1143	1465	3072 - 3081
2	3676 - 3678	1608 - 1651	879 - 928	1355	2933 - 3027
2a	3219 - 3225	1517 - 1572	1071 - 1186	1517	2938 - 3055
2b	3151 - 3167	1584 - 1637	1093 - 1192	1449	2934 - 3059
2c	3103 - 3124	1617 - 1656	1113 - 1199	1454	2933 - 3059
2d	3147 - 3165	1619 - 1672	1109 - 1183	1456	2934 - 3057
3	3231 - 3665	1485 - 1557	921 - 1059	1234	3069 - 3101
3a	3202 - 3209	1515 - 1552	1082 - 1108	1427	3066 - 3100
3b	3134 - 3150	1574 - 1608	1087 - 1106	1430	3067 - 3101
3c	3082 - 3101	1625 - 1601	1073 - 1116	1434	3101 - 3068
3d	3298 - 3303	1595 - 1637	1071 - 1098	1426	3074 - 3103
4	3671 - 3673	1617 - 1623	932	1335	3058 - 3133
4a	3176 - 3182	1564	1047 - 1141	1554	3080 - 3122
4b	3175 - 3188	1555 - 1606	1038 - 1077	1482	3079 - 3123
4c	3106 - 3127	1585 - 1623	1042 - 1110	1507	3079 - 3121
4d	3129 - 3151	1585 - 1634	1033 - 1114	1437	3078 - 3120

1a': Calculated frequencies of Fe(II) complex with ligand 1 at B3LYP/6-31+G(d,p)/(SDD for metal ion). 1b': Calculated frequencies of Co(II) complex with ligand 1 at B3LYP/6-31+G(d,p)/(SDD for metal ion).

Table 6. To obtain the nature and the energies of the electronic transitions within the investigated complexes, the first twenty low-lying excited states have been calculated. The absorption energies with first two higher oscillator strengths are considered throughout the discussion in this paper. The TD-DFT results in **Table 7** have shown that the lowest energy transition in the complexes correspond to electronic excitations from HOMO to LUMO. The absorption intensity is directly related to the dimensionless oscillator strength value and the dominant absorption bands are the transitions with highest oscillator strength.

For the first series of complexes, the most intense band was observed at: 295.02, 326.80, 216.88 and 264.83 nm for the 1a, 1b, 1c and 1d complexes respectively. As evidenced in **Figure 4(a)**, the absorption band for complex 1c has been found to be the most intense, with high oscillator strength, 0.4923. The intensities of the absorption

Table 6. Computed UV-Vis absorption bands, dominant transitions, and oscillator strengths (f) of metal 3d glyoximes complexes at B3LYP/6-31+G(d,p) with LANL2DZ for metal(II).

Molecules	Orbital transition	Energy (ev)	Wavelength (nm)	Oscillator strength	Character
1a	HOMO − 2 → LUMO + 1 (0.67)	4.2026	295.02	0.1634	ILCT/LMCT/LLCT
1b	HOMO − 2 → LUMO (0.72)	3.7938	326.80	0.0576	MLCT/LLCT
1c	HOMO − 7 → LUMO + 1 (0.62)	5.7167	216.88	0.4923	LMCT/LLCT/ILCT/d-d/MLCT
1d	HOMO − 2 → LUMO (0.56)	4.6816	264.83	0.2186	ILCT
2a	HOMO − 2 → LUMO (0.54)	3.4760	356.69	0.1588	LMCT/LLCT/ILCT
2b	HOMO − 2 → LUMO (0.59)	3.9155	316.65	0.0586	LLCT/MLCT
2c	HOMO − 8 → LUMO + 1 (0.62)	5.7857	214.29	0.4516	LMCT/LLCT/ILCT/d-d/MLCT
2d	HOMO → LUMO + 1 (0.70)	4.5480	272.61	0.1389	LLCT/ILCT
3a	HOMO − 2 → LUMO (0.45)	3.3972	364.96	0.3154	LMCT/ILCT
3b	HOMO − 1 → LUMO (0.53)	3.7523	330.42	0.1235	d-d/ILCT/LMCT
3c	HOMO − 1 → LUMO (0.64)	4.0710	304.56	0.2843	ILCT/LLCT
3d	HOMO − 10 → LUMO (0.96)	3.6437	340.27	0.1971	LMCT/LLCT/ILCT/d-d/MLCT
4a	HOMO − 4 → LUMO + 1 (0.48)	3.1790	390.02	0.2849	LMCT/LLCT/ILCT/d-d/MLCT
4b	HOMO → LUMO (0.72)	2.6979	459.55	0.0792	ILCT/LMCT
4c	HOMO − 3 → LUMO (0.66)	3.5501	349.24	0.1166	LLCT/MLCT
4d	HOMO − 6 → LUMO + 1 (0.97)	3.7972	326.52	0.1290	LMCT/ILCT/LLCT

bands of this series of complexes are in the decreasing order: 1c > 1a > 1d > 1b.

The transition energy is inversely proportional to the absorption wavelength in each case, for instance, complex 1c has a high absorption energy (5.7167 ev) corresponding to the HOMO − 7 → LUMO + 1 electronic transition, which is observed at the wavelength 216.88 nm. The molecular orbital compositions in Table 7 have revealed that 64.44% of the electron density in HOMO − 7 of 1c is localized mainly on the two chloride ligands and 61.81% of the electron density in LUMO + 1 is localized on the metal ions, hence the character for this transition is mainly ligand-to-metal charge transfer (LMCT).

For the second series of complexes containing dimethylglyoxime as one of the ligands, the maximum absorption bands appeared at: 356.69, 316.65, 214.29 and 272.61 nm for the 2a, 2b, 2c and 2d complexes respectively. It is clear from Figure 4(b) that the absorption band for complex 2c with high oscillator strength, 0.4516 is the most intense. For this series, absorption intensities decrease in the order: 2c > 2a > 2d > 2b. As such, the most intense band in 2c is due mainly to the transition HOMO − 8 → LUMO + 1. On the basis of the molecular orbital compositions in Table 7, the electron density in HOMO − 8 is localized mainly on the two chloride ligands (65.56%), and that of LUMO + 1 is localized mainly on the metal ions (62.15%), hence, the HOMO − 8 is essentially the p-type orbitals p(Cl) on the chloride ligands (donors) whereas LUMO + 1 is mainly the d-type orbital, d(Ni) on nickel(II) ion (acceptor). Therefore, the transition

Table 7. Frontier molecular orbital compositions for the ground states of metal 3d glyoximes complexes at B3LYP/6-31+G(d,p) with LANL2DZ for metal(II).

Molecules	Orbital	Index	M	2Cl⁻	L	Main bond type
1a	HOMO − 2	46	2.46	23.82	73.72	π(L) + p(Cl)
	LUMO + 1	50	16.51	2.8	80.69	π*(L) + d(Fe)
1b	HOMO − 2	47A	27.55	67.24	5.20	p(Cl) + d(Co)
	LUMO	50A	9.41	1.67	88.92	π*(L)
1c	HOMO − 7	42	17.71	64.44	17.85	p(Cl) + π(L) + d(Ni)
	LUMO + 1	51	61.81	23.18	15.01	d(Ni) + p(Cl) + π*(L)
1d	HOMO − 2	45B	1.00	5.47	93.53	π(L)
	LUMO	51B	5.46	1.08	93.45	π*(L)
2a	HOMO − 2	54	2.63	22.25	75.11	π(L) + p(Cl)
	LUMO	57	79.19	10.15	10.66	d(Fe) + π*(L) + p(Cl)
2b	HOMO − 2	55A	31.11	62.64	6.26	p(Cl) + d(Co)
	LUMO	58A	9.11	1.61	89.28	π*(L)
2c	HOMO − 8	49	15.60	65.56	18.83	p(Cl) + π(L) + d(Ni)
	LUMO + 1	59	62.15	22.34	15.51	d(Ni) + p(Cl) + π(L)
2d	HOMO	57B	6.43	80.68	12.89	p(Cl) + π(L)
	LUMO + 1	59B	6.19	1.26	92.55	π*(L)
3a	HOMO − 2	86	2.58	8.48	88.94	π(L)
	LUMO	89	76.66	9.91	13.42	d(Fe) + π*(L)
3b	HOMO − 1	88A	41.66	24.01	34.34	d(Co) + π(L)+ p(Cl)
	LUMO	90A	62.15	6.02	31.83	d(Co) + π*(L)
3c	HOMO − 1	88	9.24	20.88	69.88	π(L) + p(Cl)
	LUMO	90	7.95	1.49	90.56	π*(L)
3d	HOMO − 10	79B	17.91	61.05	21.04	p(Cl) + π(L) + d(Cu)
	LUMO	90B	54.44	28.18	17.38	d(Cu) + p(Cl) + π*(L)
4a	HOMO − 4	57	14.33	72.88	12.78	p(Cl) + d(Fe) + π(L)
	LUMO + 1	63	68.04	8.30	23.66	d(Fe) + π*(L)
4b	HOMO	61B	2.61	4.50	92.89	π(L)
	LUMO	62B	13.47	2.19	84.34	π*(L) + d(Co)
4c	HOMO − 3	59	24.26	69.45	6.10	p(Cl) + d(Ni)
	LUMO	63	7.00	1.22	84.38	π*(L)
4d	HOMO − 6	56B	17.84	61.48	20.36	p(Cl)
	LUMO + 1	64B	57.12	28.23	14.41	d(Cu) + p(Cl) + π*(L)

character of the most intense band in 2c is principally ligand-to-metal charge transfer (LMCT).
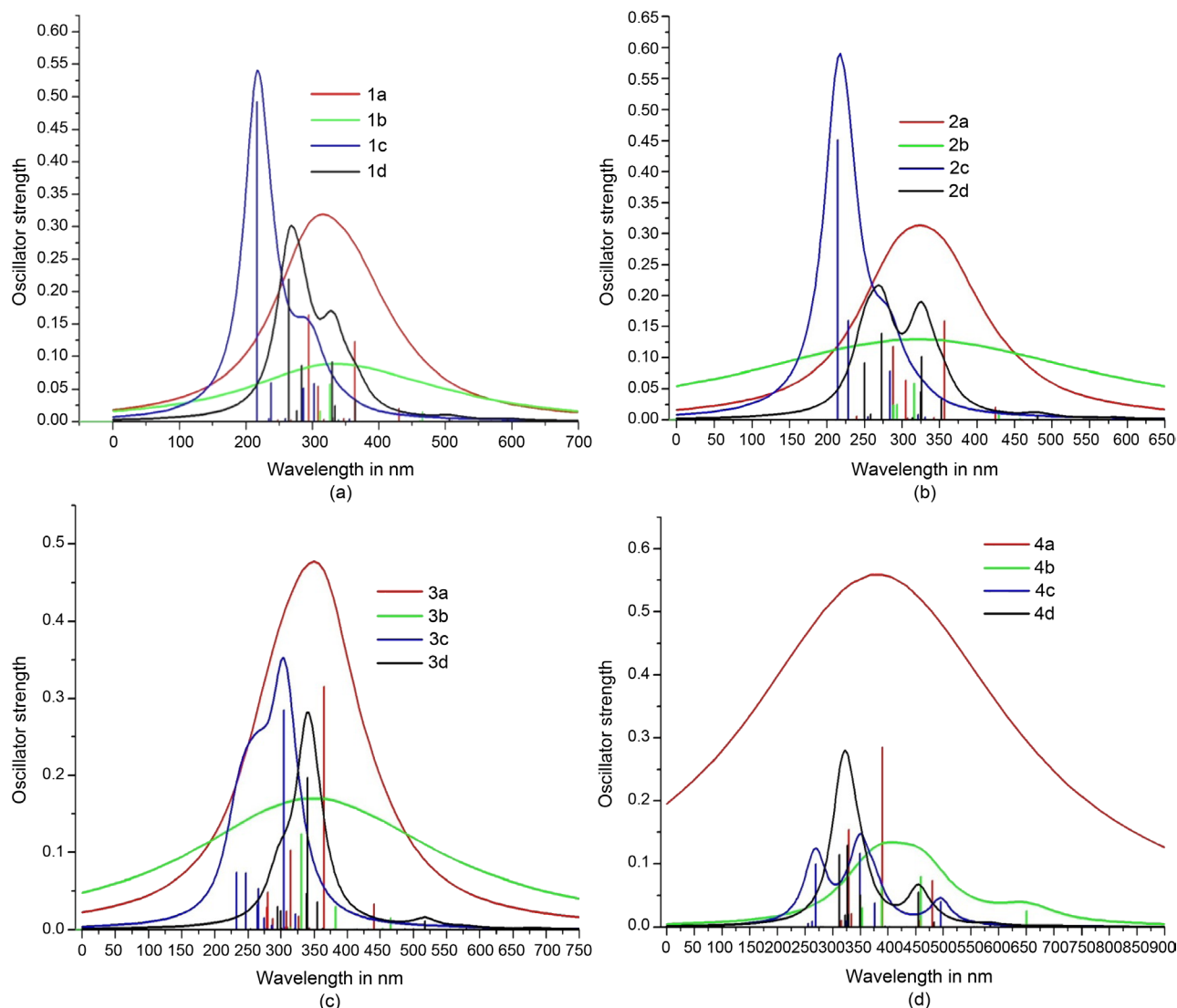
Figure 4. Schematic of calculated electronic transitions of glyoximes complexes.

In the case of the third series, the maximum absorption bands are: 364.96, 330.42, 304.56 and 340.27 nm corresponding to the 3a, 3b; 3c and 3d complexes respectively. Hence, the most intense band with high oscillator strength (0.3154) is exhibited by 3a. The intensities of the dominant transitions in this series can be classified in the increasing order: 3a > 3c > 3d > 3b (Figure 4). The maximum absorption band in 3a corresponds to the transition HOMO – 2 → LUMO. From the molecular orbital compositions in Table 7, it is clear that the electron density in HOMO – 2 is mainly localized on the diphenylglyoxime ligand (88.94%) and that of the LUMO is similarly localized on the central metal (76.66%). As such, the HOMO – 2 is a π-donor and the LUMO is the d-type orbital of Fe. The main transition character of the most intense absorption band in 3a is ligand-to-metal charge transfer (LMCT).

For the last series of complexes studied, the maximum absorption bands are respectively 390.02, 459.55, 349.24 and 326.52 nm for the 4a; 4b; 4c and 4d complexes. Clear

from Table 7, the highest absorption energy was observed for the 4a complex (3.1790 eV) corresponding to the HOMO − 4 → LUMO + 1 transition. From the molecular orbital composition analysis result in Table 7, it is obvious that the electron density in HOMO − 4 is mainly localized on the two chloride ligands (72.88%) and that of the LUMO + 1 is localized mainly on the metal ion which has contributed 68.04% of it, and the ligands (L) that have contributed 23.66%. It can be concluded from these results that the most intense electronic band in 4d has a mixed ligand-to-metal charge transfer (LMCT) and ligand-to-ligand charge transfer (LLCT) character (Table 6).

4. Conclusion

DFT and TD-DFT calculations were used to investigate the molecular properties of some 3d metal (II) chloride glyoxime complexes. The optimized geometries of the complexes studied revealed a nearly square planar geometry around the central metal ion in each complex. Our results showed the existence of hydrogen bonds between the two OH groups of glyoxime and the two chloride ligands in all complexes investigated, which significantly contribute toward the stabilization of the complexes. As a general observation for all the metal ions studied, the ligands showed the greatest affinity toward the nickel(II) ion and the least affinity toward copper(II) ion. For the complexes studied, all complexation reactions were found to be thermodynamically feasible and exothermic. Natural population analysis showed the possibility of ligand-to-metal charge transfer. Electronic absorption bands obtained in the UV/Visible region have been attributed mainly to MLCT, LMCT and d-d electronic transitions involving metal-based orbitals.

Acknowledgements

References

[1]   Rija, A., Bulhac, I., Coropceanu, E., Gorincioi, E., Calmîc, E. and Barba, O. (2011) Bologa-synthesis and Spectroscopic Study of some Coordinative Compounds of Co(III), Ni(II) and Cu(II) with Dianiline- and Disulfanilamideglyoxime. *Chemistry Journal of Moldova*, **6**, 73-78.

[2]   Smith, A.G., Tasker, P.A. and White, D.J. (2003) The Structures of Phenolic Oximes and their Complexes. *Coordination Chemistry Reviews*, **241**, 61-85.
http://dx.doi.org/10.1016/S0010-8545(02)00310-7

[3]   Blower, P.J. (1997) Small Coordination Complexes as Radiopharmaceutical for Cancer Targeting. *Transition Metal Chemistry*, **23**, 109-112.
http://dx.doi.org/10.1023/A:1006926505754

[4]   Karapcin, F. and Arabali, F. (2006) Synthesis and Characterization of 4-Arylaminobi-Phenylglyoximes and Their Complexes. *Journal of the Chilean Chemical Society*, **51**, 982-

985.

[5] Chaudhuri, P. (2003) Homo- and Hetero-Polymetallic Exchange Coupled Metal-Oximates. *Coordination Chemistry Reviews*, **243**, 143-190. http://dx.doi.org/10.1016/S0010-8545(03)00081-X

[6] Kurtoglu, M. and Baydemir, S.A. (2007) Studies on Mononuclear Transition Metal Chelates Derived from a Novel (E,E)-Dioxime: Synthesis, Characterization and Biological Activity. *Journal of Coordination Chemistry*, **60**, 655-665. http://dx.doi.org/10.1080/00958970600896076

[7] Serin, S. (2001) New Vic-Dioxime Transition Metal Complexes. *Transition Metal Chemistry*, **26**, 300-306. http://dx.doi.org/10.1023/A:1007163418687

[8] Schrauzer, G.N. (1976) New Developments in the Field of Vitamin B12: Reactions of the Cobalt Atom in Corrins and in Vitamin B12 Model Compounds. *Angewandte Chemie International*, **15**, 417-426. http://dx.doi.org/10.1002/anie.197604171

[9] Alper, T.O., Gazi, I., Hasene M., Tuncer, H. and Nagihan A. (2009) A Co(III) Complex with a Tridentate Amine-Imine-Oxime Ligand from 1,2,3,4-Tetrahydroquinazoline: Synthesis, Crystal Structure, Spectroscopic and Thermal Characterization. *Journal of Coordination Chemistry*, **62**, 1005-1014. http://dx.doi.org/10.1080/00958970802345831

[10] Gök, Y. and Kantekin, H. (1997) Synthesis and Characterization of Novel (E,E)-Dioximes and Its Mono- and Heterotrinuclear Complexes. *Acta Chemica Scandinavica*, **51**, 664-671. http://dx.doi.org/10.3891/acta.chem.scand.51-0664

[11] Kuse, S. Motomizu, S. and Toei, K. (1974) Diketonedioxime Compounds as Analytical Reagents for the Spectrophotometric Determination of Nickel. *Analytica Chimica Acta*, **70**, 65-76. http://dx.doi.org/10.1016/S0003-2670(01)82911-1

[12] Mercimek, B., Ozler, M.A., Irez, G. and Bekaroglu, O. (1999) Synthesis of a Novel Heterocyclic Dioxime and its Mononuclear Complexes with Ni(II), Co(II), Cu(II), Zn(II), Cd(II) and Hg(II). *Synthesis and Reactivity in Inorganic and Metal-Organic*, **29**, 513-524. http://dx.doi.org/10.1080/00945719909349466

[13] Kurita, K. (1998) Chemistry and Application of Chitin and Chitosan. *Polymer Degradation and Stability*, **59**, 117-120. http://dx.doi.org/10.1016/S0141-3910(97)00160-2

[14] Soga, S., Sharma, S., Shiotsu, Y., Shimizu, M., Tahara, H., Yamaguchi, K., Ikuina, Y., Murakata, C., Tamaoki, T., Kurebayashi, J., Schulte, T., Neckers L. and Akinaga, S. (2001) Stereospecific Antitumor Activity of Radicicoloxime Derivatives. *Cancer Chemotherapy Pharmacology*, **48**, 435-445. http://dx.doi.org/10.1007/s002800100373

[15] Underhill, A.E., Watkins D.M. and Petring, R. (1973) Electrical Conduction Properties of Ni(dpg)$_2$I, Ni(dpg)$_2$Br, and Pd(dpg)$_2$I (Where dpg = Diphenylglyoxime). *Journal* of *Inorganic and Nuclear Chemistry*, **9**, 1269-1273. http://dx.doi.org/10.1016/0020-1650(73)80009-1

[16] Park, H.J., Lee, K., Park, S.J., Ahn, B., Lee, J.C., Cho, H. and Lee, K.I. (2005) Identification of Antitumor Activity of Pyrazole Oxime Ethers. *Bioorganic and Medicinal Chemistry Letters*, **13**, 3307-3312. http://dx.doi.org/10.1016/j.bmcl.2005.03.082

[17] Thomas, T.W. and Underhill, A. E. (1972) Metal-metal Interactions in Transition-Metal Complexes Containing Infinite Chains of Metal Atoms. Chemical *Society Reviews*, **1**, 99-120. http://dx.doi.org/10.1039/CS9720100099

[18] Hayati, S., Muzaffer, C. and Mustafa, M. (2005) Potentiometric and Theoretical Studies of Stability Constants of Glyoxime Derivatives and Their Nickel, Copper, Cobalt and Zinc Complexes. *Acta Chimica Slovenica*, **52**, 317-322.

[19] Ulku, S., Omer, D., Ercan, T. and Ayhan, O. (2012) Magnetic Properties of Single Crystal Alpha-Benzoinoxime: An EPR Study. *Radiation Physics and Chemistry*, **81**, 146-151. http://dx.doi.org/10.1016/j.radphyschem.2011.08.013

[20] Frisch, M.J., Trucks, G.W., Schlegel, H.B., Scuseria, G.E., Robb, M.A., Cheeseman, J.R., Scalmani, G., Barone, V., Mennucci, B., Petersson, G.A., Nakatsuji, H., Caricato, M., Li, X., Hratchian, H.P., Izmaylov, A.F., Bloino, J., Zheng, G., Sonnenberg, J.L., Hada, M., Ehara, M., Toyota, K., Fukuda, R., Hasegawa, J., Ishida, M., Nakajima, T., Honda, Y., Kitao, O., Nakai, H., Vreven, T., Montgomery Jr., J.A., Peralta, J.E., Ogliaro, F., Bearpark, M., Heyd, J.J., Brothers, E., Kudin, K.N., Staroverov, V.N., Kobayashi, R., Normand, J., Raghavachari, K., Rendell, A., Burant, J.C., Iyengar, S.S., Tomasi, J., Cossi, M., Rega, N., Millam, J.M., Klene, M., Knox, J.E., Cross, J.B., Bakken, V., Adamo, C., Jaramillo, J., Gomperts, R., Stratmann, R.E., Yazyev, O., Austin, A.J., Cammi, R., Pomelli, C., Ochterski, J.W., Martin, R.L., Morokuma, K., Zakrzewski, V.G., Voth, G.A., Salvador, P., Dannenberg, J.J., Dapprich, S., Daniels, A.D., Farkas, O., Foresman, J.B., Ortiz, J.V., Cioslowski, J. and Fox, D.J. (2009) Gaussian 09, Revision A.02. Gaussian, Inc., Wallingford.

[21] Casida, M.E. (1995) In Recent Advances in Density Functional Methods, Part I. World Scientific, Singapore City.

[22] Gross, E.K.U., Dobson, J.F. and Petersilka, M. (1996) Introduction Density Functional Theory II. Springer, Heidelberg.

[23] Mariappan, G. and Sundaraganesan, N. (2014) Spectral and Structural Studies of the Anti-Cancer Drug Flutamide by Density Functional Theoretical Method. *Spectrochimica Acta Part A*, **117**, 604-612. http://dx.doi.org/10.1016/j.saa.2013.09.043

[24] Lee, C., Yang W. and Parr, R.G. (1988) Local Softness and Chemical Reactivity in Molecules CO, SCN$^-$ and H_2CO. *Journal of Molecular Structure*, **163**, 305-313. http://dx.doi.org/10.1016/0166-1280(88)80397-X

[25] Parr, R.G. and Pearson, R.G. (1983) Absolute Hardness: Companion Parameter to Absolute Electronegativity. *Journal of the American Chemical Society*, **105**, 7512-7516. http://dx.doi.org/10.1021/ja00364a005

[26] Parr, R.G., Donnelly, R.A., Levy M. and Palke, W.E. (1978) Electronegativity—The Density Functional Viewpoint. *Journal of Chemical Physics*, **68**, 3801-3807. http://dx.doi.org/10.1063/1.436185

[27] Parr, R.G. and Yang, W. (1988) Density Functional Theory of Atoms and Molecules. Oxford Science Publications, New York.

[28] Bayrak, C. and Bayari, S.H. (2010) Vibrational and DFT Studies of Creatinine and Its Metal Complexes. *Hacettepe Journal of Biology and Chemistry*, **38**, 107-118.

[29] Cramer, C.J. (2004) Essentials of Computational Chemistry: Theories and Models.4th Edition, John Wiley & Sons Ltd., West Sussex.

[30] Lewars, E.G. (2011) Computational Chemistry: Introduction to the Theory and Applications of Molecular and Quantum Mechanics. 2nd Edition, Springer, New York. http://dx.doi.org/10.1007/978-90-481-3862-3

[31] Foresman, J.B. and Frisch, A. (1996) Exploring Chemistry with Electronic Structure Methods. 2nd Edition, Gaussian Inc., Pittsburgh.

[32] Panicker, C.Y., Varghese, H.T., Ambujakshan, K.R., Mathew, S., Ganguli, S., Nanda, A.K. and Van Alsenoy, C. (2009) FT-IR and FT-Raman Spectra and *ab Initio* Calculations of 3-{[(2-Hydroxyphenyl)Methylene]Amino}-2-Phenylquinazolin-4(3H)-One. *Journal of Raman Spectroscopy*, **40**, 1262-1273. http://dx.doi.org/10.1002/jrs.2276

[33] Teimouri, A.N., Chermahini, A., Taban, K. and Dabbagh, H. (2009) Experimental and CIS, TD-DFT, *ab Initio* Calculations of Visible Spectra and the Vibrational Frequencies of Sulfonylazide-Azoic Dye. *Spectrochimica Acta Part A*, **72**, 369-377. http://dx.doi.org/10.1016/j.saa.2008.10.006

Scientific Research Publishing

Submit or recommend next manuscript to SCIRP and we will provide best service for you:

Accepting pre-submission inquiries through Email, Facebook, LinkedIn, Twitter, etc.
A wide selection of journals (inclusive of 9 subjects, more than 200 journals)
Providing 24-hour high-quality service
User-friendly online submission system
Fair and swift peer-review system
Efficient typesetting and proofreading procedure
Display of the result of downloads and visits, as well as the number of cited articles
Maximum dissemination of your research work

Submit your manuscript at: http://papersubmission.scirp.org/
Or contact cc@scirp.org

Scientific Research Publishing